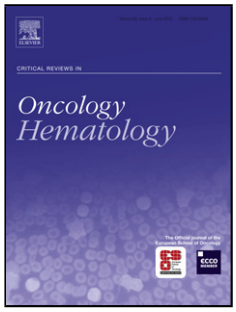

Recommendation for the contouring of limbic system in patients receiving radiation treatment: A pictorial review for the everyday practice and education

Claudia Sorce, Agnieszka Chalaszczyk, Francesca Rossi, Letizia Ferella, Gianmarco Grimaldi, Alessandra Splendiani, Domenico Genovesi, Francesco Marampon, Ester Orlandi, Alberto Iannalfi, Carlo Masciocchi, Giovanni Luca Gravina

PII: S1040-8428(21)00017-2

DOI: https://doi.org/10.1016/j.critrevonc.2021.103229

Reference: ONCH 103229

To appear in: *Critical Reviews in Oncology / Hematology*

Received Date: 23 June 2020

Revised Date: 9 December 2020

Accepted Date: 16 January 2021

Please cite this article as: Sorce C, Chalaszczyk A, Rossi F, Ferella L, Grimaldi G, Splendiani A, Genovesi D, Marampon F, Orlandi E, Iannalfi A, Masciocchi C, Gravina GL, Recommendation for the contouring of limbic system in patients receiving radiation treatment: A pictorial review for the everyday practice and education, *Critical Reviews in Oncology / Hematology* (2021), doi: https://doi.org/10.1016/j.critrevonc.2021.103229

Recommendation for the contouring of limbic system in patients receiving radiation treatment: A pictorial review for the everyday practice and education

Claudia Sorce M.D.[1], Agnieszka Chalaszczyk M.D[5], Francesca Rossi M.D[1], Letizia Ferella M.D.[7], Gianmarco Grimaldi M.D.[1], Alessandra Splendiani M.D.[2], Domenico Genovesi M.D.[6], Francesco Marampon M.D., Ph.D.[4], Ester Orlandi M.D.[5], Alberto Iannalfi M.D.[5], Carlo Masciocchi M.D.[3], Giovanni Luca Gravina M.D., Ph.D[1]

[1]Department of Biotechnological and Applied Clinical Sciences, Division of Radiotherapy. Laboratory of Radiobiology, University of L'Aquila

[2]Department of Biotechnology & Applied Clinical Science, University of L'Aquila, Division of Neuroradiology, L'Aquila, Italy.

[3]Department of Biotechnology & Applied Clinical Science, University of L'Aquila, Division of Radiology, L'Aquila, Italy

[4]Department of Radiation Oncology, Policlinico Umberto I Hospital, Sapienza, University of Rome, Rome, Italy

[5]Clinical Department, National Center for Oncological Hadrontherapy (CNAO), Pavia.

[6]Department of Radiotherapy , 'SS Annunziata' Hospital 'G. D'Annunzio' University , Chieti , Italy;

[7]Radiation Oncology, ThomoTherapy Unit, Hospistal of Aosta, Italy

Corresponding author:

Prof. Giovanni Luca Gravina; Department of Biotechnological and Applied Clinical Sciences, Division of Radiotherapy. Laboratory of Radiobiology, University of L'Aquila; Via Vetoio, 67100 L'Aquila, Italy; email address: giovanniluca.gravina@univaq.it, phone number:+390862368988

Abstract

Aims: The limbic circuit (LC) is devoted to linking emotion to behavior and cognition. The injury this system results in post-RT cognitive dysfunction. The aim of this study is to create the first radiation oncologist's practical MR-based contouring guide for the delineation of the LC for the everyday clinical practice and education. **Methods:** An anonymized diagnostic 3.0T T1-weighted BRAVO MRI sequence from a healthy patient with typical brain anatomy was used to delineate LC. For each structure key anatomical contours were completed by radiation oncologists, along with a neuro-radiologist to generate the final version of the LC atlas. **Results:** a step-by-step MR-based atlas of LC was created. Key structures of the LC, such as, cingulate gyrus, fornix, septal region, mammillary bodies, thalamus and the hippocampal-amygdala formation were contoured. **Conclusions:** This article provides the recommendations for the first contouring atlas of LC in the setting of patients receiving RT and education.

Key words: Radiotherapy, oncology, limbic system, toxicity, contorting atlas, education

1. Introduction

Primary and metastatic brain tumors as well as nasopharyngeal (NPC) and sinunasal carcinomas are currently managed by integrated treatments. In these clinical scenarios radiotherapy (RT) plays an essential role. However, radiation-induced brain injury and subsequent neurocognitive (NC) decline is a major cause of morbidity in long term cancer survivors [1, 2]. This is because central nervous system (CNS) represents the planned target (brain tumors) of RT or it is incidentally included within the RT fields. Thanks to the technological improvements in RT system technology, it is now possible to selectively spare important brain structures that may contribute to cognitive decline after both partial and whole-brain RT (WBRT) [3-21]. Proton-therapy may also provide an effective way of minimizing dose to hippocampi and other critical regions of

neurogenesis in subjects suffering from low and high grade gliomas [21]. Many brain regions, other than hippocampus, are involved in the post-RT NC decline. They include the limbic circuit (LC) which is a complex group of interconnected subcortical and cortical regions devoted to linking emotion and visceral states to behavior and cognition [22]**.** The sparing of LC during RT has been less intensively investigated than hippocampus sparing and the literature on this topic is somewhat inconsistent. Three dosimetric studies have demonstrated the feasibility of LC sparing during WBRT or partial-brain RT in high-grade gliomas [23-26]. However, other important requirements are needed to ensure the prompt implementation of the LC sparing in the everyday clinical practice. The first one concerns the careful selection of patients who can benefit greatly from this sparing approach. This aspect is closely related to a detailed knowledge of the incidence of brain metastases within the LC. Evidence indicates that metastatic involvement of this circuit is uncommon in the population with brain metastases, with the lowest incidence occurring in subjects with oligometastatic brain disease [26-30]. This has important clinical implications since the risk of post-RT NC decline increases over time and the oligometastatic population, having durable long-term survival, can benefit greatly from a LC sparing approach. Furthermore, the sparing of this system could have even a more clinically- relevant impact on patients affected by primary brain tumors receiving focal RT especially for benign and low grade tumors.

However, the major current drawback is the lack of a contouring guide of limbic structures for planning and educational purpose. Aim of this study is to create the first proposal radiation oncologist's practical MR-based contouring guide for the delineation of the LC for the everyday clinical practice and education.

2. Materials and methods

Atlas development information was sought from (i) textbooks [22, 31-33], (ii) IMAIOS e-anatomy [34] and (iii) key articles describing the structures of LC anatomy and sulci [35-37]. A diagnostic 3-Tesla Magnetic resonance imaging (MRI) T1-weighted BRAVO sequence of a male subject without

pathological findings was anonymized and used to delineate the LC. The MRI study was carried out by using a three Tesla (Discovery MR, General Electric Medical Systems, Erlangen, Germany) scan, using a 32-channel head coil. Structural T1w volumes were acquired using a three-dimensional magnetization-prepared fast spoiled gradient echo sequence (144 sagittal partitions; TR 6.6 ms; TE 2.3 ms; TI 1100 ms; flip angle 7◦ ; voxel size 1 × 1 × 1 mm3). This specific sequence was selected due to its superior soft tissue contrast. It was acquired in the three MR planes (standard axial, sagittal and coronal reconstructions). MR was obtained in the supine position with the head in a neutral position. During a multi-disciplinary session, two radiation expert oncologists (XXX and XX) discussed the delineation of the LC structures in collaboration with an expert neuro-radiologist (XX) and came to consensus on a first draft atlas. Contours of each structure were then reviewed in detail by XX, XX, XX, XX and XX. The Elekta's Monaco version 5.11 software (ELEKTA CMS, INC., Stockholm, Sweden) was used to delineate the different parts of the LC. The approved first draft atlas was shared with all other coauthors for assessment, input, and final approval. The written informed consent for the use of MRI scan was obtained and the study was approved by the Internal Review Board of our University.

3. Results

3.1 Delineation on axial slices of hippocampal-amygdala formation and mammillary bodies

The hippocampal formation and the amygdala are contoured as a single structure and is named hippocampal-amygdala formation. It includes the hippocampus proper, the dentate gyrus, the alveus, the fimbria, the amygdala and the uncus. The hippocampal-amygdala formation with the mammillary bodies were displayed on 15 not consecutive slices on a caudal to cranial direction (Figure 1).

Slice 1: Begin contouring the hippocampal-amygdala complex where the temporal horn of the lateral ventricle is well resolved. At this level the temporal horn is not jet visible and the hippocampal-amygdala complex is not contoured.

Slice 2: Contour the hypointense gray matter medially to the temporal horn. The hippocampal-amygdala formation is anteriorly and laterally marked by the white matter of the superior temporal gyrus and anteriorly and medially by the most medial part of the gray matter of temporal lobe. In order to improve consistency and reproducibility, a portion of the entorhinal cortex was included in the most medial part of the hippocampal-amygdala formation. This border is marked by the cerebrospinal fluid of the pontine cistern. Posteriorly this complex is marked by the white matter of parahippocampal gyrus. The amygdala is displayed as the dashed yellow boundary.

Slice 3: The hippocampal-amygdala complex is anteriorly marked by the white matter of superior temporal gyrus and by the most medial part of the gray matter of temporal lobe. The medial border is marked by the cerebrospinal fluid of the anterior basal cistern. On an anterior-posterior direction, the lateral border is marked by the white matter of the temporal lobe and by the temporal horn of the lateral ventricle, respectively. Posteriorly this complex is marked by the white matter of parahippocampal gyrus.

Slice 4: At this level the hippocampal-amygdala formation is anteriorly surrounded by the cerebrospinal fluid of anterior basal cistern.

Slice 5-6: On an anterior-posterior direction, the lateral border is marked by the white matter of the temporal lobe and by the temporal horn of the lateral ventricle, respectively. Medially the complex is surrounded anteriorly by the cerebrospinal fluid of interpeduncular cistern and posteriorly by the cerebrospinal fluid of the ambient cistern. Posteriorly this complex is marked by the white matter of the parahippocampal gyrus.

Slice 7: The hippocampal-amygdala formation is anteriorly marked by the cerebrospinal fluid of the insular cistern, laterally by the white matter of the temporal lobe and by the temporal horn of the lateral ventricle. Posteriorly this formation is marked by the white matter of the parahippocampal gyrus. Medially the hippocampal-amygdala formation is marked by the crural cistern in its most anterior part and by the ambient cistern in its most posterior part.

Slice 8: At this level the most cranial aspect of the mammillary bodies is displayed. They are anteriorly marked by the supraoptic recess and posteriorly by interpeduncular cistern. Laterally this structure is surrounded by the cerebrospinal fluid of the insular cistern.

Slice 9: The hippocampal-amygdala formation is anteriorly marked the cerebrospinal fluid of the insular cistern. On an anterior-posterior direction, the lateral border is marked by the withe matter of the temporal lobe and by the temporal horn of the lateral ventricle, respectively. Posteriorly this formation is marked by the white matter of the parahippocampal gyrus. Medially the hippocampal-amygdala formation is marked by the crural cistern in its most anterior part and by the ambient cistern in its most posterior part. At this level the mammillary bodies are well resolved and are anteriorly marked by the supraoptic recess and posteriorly by interpeduncular cistern. Laterally this structure is surrounded by the cerebrospinal fluid of the insular cistern

Slice 10: At this level the contouring of the hippocampal-amygdala formation is divided in an anterior and posterior portion. Anteriorly the most inferior part of the amygdala and uncus is contoured. Posteriorly the body-tail of the hippocampus is contoured. At this level the amygdala is anterior-medially surrounded by the cerebrospinal fluid of the insular cistern and latero-posteriorly is marked by the white matter of the temporal lobe. The hippocampus is marked laterally by the atrium of the lateral ventricle, posteriorly by the white matter of parahippocampal gyrus and medially by the cerebrospinal fluid of the ambient cistern.

Slice 11: At this level the contouring of amygdala and the uncus are still displayed. These structures are in close anatomical relationship with the optic tracts.

Slice 12: The amygdala and the uncus are no longer displayed. Stop the contouring of these structures when the optic tracts are no longer visible.

Slice 13-15: The hippocampal tail remains posterior to the pulvinar of the thalamus and it is laterally surrounded by the cerebrospinal fluid of the atrium of lateral ventricle and medially by the ambient cistern.

Slice 16: At this level the hippocampal tail is no longer displayed. Stop the contouring of this structure when the corpus callosum appears.

3.2 Delineation on coronal and axial slices of fornix and septal region

A step-by step delineation of the fornix and the septal region is provided on a coronal plane. The anatomical limits of these structures are easier displayed on this plane (Figure 2). The fornix and the septal region are displayed on 12 not consecutive coronal slices on a posterior to anterior direction.

3.2.1 The Fornix

Slice 1: Begin contouring the crus of the fornix at the most posterior appearance of hippocampus (tail of hippocampus) where the hyperintense fimbria is visible. In order to assure a better consistency during contouring, contour the crus of fornix as a 2 mm bundle from the fimbria of hippocampus to the middle third of the lateral surface (ventricular side) of the splenium of the corpus callosum.

Slice 2: Continue to contour in a posterior-anterior direction on a coronal plane form the fimbria of hippocampus to the middle third of the lateral border (ventricular side) of the splenium of the corpus callosum. In this slice the crus of fornix appears in all its length.

Slice 3: Continue to contour in a posterior-anterior direction on a coronal plane. When the pulvinar of the thalamus is well resolved and the splenium of the corpus callosum disappears, the lateral

aspect of the crus of the fornix is in close anatomical relationship with thalamus/choroid plexus. Crus of the fornix ends medially and superiorly at the level of lamina of septum pellucidum.

Slice 4: Continue to contour in a posterior-anterior direction on a coronal plane. At this level the crus of the fornix is superiorly suspended at the corpus callosum by the septum pellucidum. The thalamus at this level is well resolved.

Slice 5: On both sides the crus of fornix continues anteriorly and merges to form the body of the fornix. This structure is superiorly suspended at the corpus callosum by the septum pellucidum. The inferior part of the body of the fornix comes into close relationship with the choroid plexus and third ventricle.

Slice 6-7: The body of the fornix is divides, at the level of the interventricular foramen of Monro, into two halves denominated the columns of the fornix. Each column is medially delimited by the third ventricle and laterally by the internal capsule passes through the hypothalamus and reach the mammillary bodies.

Slice 8: When the mammillary bodies disappear the most inferior aspect of columns of the fornix ends just laterally to the roof of the third ventricle. The columns of the fornix stopped just before the appearance of the anterior commissure.

3.2.2 Septal region

Slice 9: As previously described the columns of the fornix stops just before the appearance of the anterior commissure. When the anterior commissure is well resolved columns of the fornix continues anteriorly in the septal region. The septal region is superiorly suspended from the corpus callosum by the septum pellucidum. Inferiorly it lies on the anterior commissure and laterally is bounded by two parallel vertical lines drawn through the most inferio-medial aspect of each lateral ventricle.

Slice 10-11: The septal region extends anteriorly and divides into two halves. It is superiorly suspended from the corpus callosum by the septum pellucidum. As in the slice 9, this structure is laterally defined by two parallel vertical lines through the most inferio-medial aspect of each lateral ventricle. Inferiorly it ends at the base of the brain and medially confines with the cisterna of the lamina terminalis.

Slice 12: In order to assure a better consistency during contouring, the septal region stopped when the infundibulum of the third ventricle disappears. This is a representative slice anterior to septal region in which neither septal gray matter nor the infundibulum of the third ventricle is visible.

An additional slice-by-slice illustration of the anatomical landmarks on an axial plane was also provided (Figure 3).

3.3 Preliminary anatomical information for contouring of cingulate gyrus (CG)

In this atlas both the gray (GM) and the white matter (WM) of the CG is contoured. For an accurate CG contouring the precise localization of sulci bordering this structure is essential. Below is provided a detailed description of the procedures for the identification of sulci on a sagittal plane (Figure 4).

Slice 1: On a sagittal plane, individuate the medial aspect of the hemisphere on a slice where the CG is well visible [45, 46]. At this level the main part of cingulate sulcus (CingS) separates the anterior-superior part of the GC from the paracingulate gyrus (PCG), the pre-motor cortex (MC) and the precentral lobe (PC). The CingS parallels the anterior and middle parts of the corpus callosum. It originates from the ventral surface of the genu of corpus callosum and, approximately above the splenium of the corpus callosum, curves upward into the parietal lobe to become the marginal ramus (MR) (pars marginalis of the CingS) [45,46]. Small accessory sulci originate from the main CingS and penetrate dorsally in the medial aspect of the PCG, the MC and the PG. The

anterior part of CingS may occasionally contain a secondary inner sulcus (Intracingulate sulcus) (white line) running within the GC. Due to the rarity of this variant the intracingulate sulcus is not used to delineate the anterio-superior border of the GC [45, 46].

Slice 2: Individuate the subparietal sulcus (SBPS). At the midline sagittal surface of the brain this sulcus posteriorly continues the curve of the CingS around the posterior part of the CG. A number of small accessory branches rise form this sulcus and superiorly run in the precuneus [45, 46].

Slice 3: Visualize the callosal sulcus (CAS) immediately above the dorsal surface of the corpus callosum. This sulcus begins anteriorly from the most ventral slice of the genu of corpus callosum and ends posteriorly to the splenium of corpus callosum [45, 46]. This sulcus marks the ventral (inferior) aspect of the CG.

3.4 Delineation on sagittal Slices of CG

A step-by step delineation of the CG, with the detailed description of the anatomical boundaries, is provided on a sagittal plane since the limit of this structure is easier displayed on this plane (Figure 5).

Slice 1: Begin contouring at the midline sagittal surface of the brain on a slice where the CingS, the MR, the SBPS and the CAS are well visible (see the figure 4). CG boundaries are anteriorly and dorsally (superiorly) the CingS. The CingS contributes with the subparietal sulcus (SBPS) to delimit posteriorly the CG. When observed on a sagittal plane, these two sulci are discontinuous in about half of the subjects and cannot be used as are to consistently delineate the posterior aspect of the CG. In order to improve consistency and reproducibility of the contouring of this border, an arbitrary limit was created (see the enlarged detail in the slice 1). It is defined by a curved line (white dotted line) joining the emergence of the MR from the CingS with the splenium of corpus callosum. This line proceeds along the inferior curved aspect of the SBPS (white arrows) joining

with a straight line (red dotted line) passing for the most inferior aspect of SBPS. Inferiorly, the CAS with the dorsal surface of corpus callosum defines the inferior border of the CG.

Slice 2. : Continue contouring in lateral direction on a sagittal plane. The CingS and the CG in their anterior-dorsal part are easily visible.

Slice 3-4: Continue contouring in lateral direction. The WM of the CG and the thalamus are well resolved.

Slice 5-6: Continue contouring in lateral direction. The CG is mainly composed of WM. The MR and the SBPS are still well resolved posteriorly.

Slice 7: Continue contouring in lateral direction. The CAS begins to disappear in its middle-anterior portion and the limit between the CG and the corpus callosum is no longer visible (see enlarged detail). At this level the inferior limit of CG is marked by a line drawn 5 mm inside the gray/white matter interface (see white arrows in the enlarged detail). This line will mark the inferior limit of CG where the CAS is no longer visible (dotted red line). Where the CAS is visible it will continue to mark the inferior limit of CG (continuous red line).

Slice 8: Continue contouring in lateral direction. Marks the inferior limit of CG where the CAS is not visible as detailed in the slice 7. The inferior aspect of SBPS marks the posterior-inferior border of CG along an imaginary straight line (red dotted line) passing for this anatomical point (see enlarged detail).

Slice 9: Continue contouring in lateral direction. The CG thickness is reducing and the MS and the SBPS are still well resolved posteriorly.

Slice 10: Continue contouring in lateral direction. The anterior border of CG is moving back and it is marked by the most anterior aspect of CingS.

Slice 11: Stop the contouring once the SBPS and/or the CingS disappear. In this slice neither the CingS nor the SBPS are visible.

3.5 Delineation on coronal Slices of thalamus

A step-by step delineation of the thalamus, with the detailed description of the anatomical boundaries, is provided on a coronal plane since the limits of this structure is easily identifiable on this plane. The Thalamus is displayed on 14 not consecutive coronal slices on an anterio-posterior direction (Figure 6).

Slice 1: This is a representative slice anterior to thalamus. At this level the thalamus is not visible and the mammillary bodies and the columns of the fornix are well resolved.

Slice 2: Begin contours the thalamus when the mammillary bodies are no longer visualized. In this slice the anterior aspect of the thalamus is well resolved and the mammillary bodies disappear. Mammillary bodies are easily identifiable in a coronal plane and the use of these anatomic landmarks in defining the anterior limit of the thalamus improves consistency and reproducibility of the contouring.

Slice 3-6: Continue contouring in an anterio-posterior direction. The thalamus is medially and inferiorly marked by the third ventricle. Superiorly the thalamus is marked by the fornix and the floor of the lateral ventricles. Laterally the internal capsule borders the thalamus.

Slice 7-8: Continue contouring in an anterior-posterior direction. The thalamus is medially marked by the third ventricle and the superior cerebellar peduncle, superiorly by the crus of the fornix and by the floor of the lateral ventricles, inferiorly by the quadrigeminal cistern and laterally by the internal capsule. The appearance of the medial (MGN) and lateral (LGN) geniculate nuclei determine an evident change in the shape of the inferior border of the thalamus.

Slice 9-10: continue contouring in an anterio-posterior direction. The thalamus is medially and inferiorly marked by the quadrigeminal cistern and superiorly by the crus fornix and floor of lateral ventricle. The lateral border is defined by the internal capsule. In this slice the MGN and LGN are no longer visualized.

Slice 13: In this slices the thalamus is displayed between the quadrigeminal cistern and the crus of the fornix. The crus is characteristically visualized diagonally for its whole length.

Slice 14: This is the slice posterior to thalamus. The thalamus is no longer visualized.

An additional slice-by-slice illustration of the anatomical landmarks of the thalamus is provided on an axial plane (Figure 7).

4. Discussion

Sparing the hippocampus, which is an important structure of LC, has proven its positive effect on the preservation of the cognitive function [3-9,]. However, even without hippocampal damage, the injury of other limbic structures, with their afferent and efferent WM pathways, results in post-RT cognitive dysfunction [38-41]. The assessment of the radiation sensitivity of structures belonging to LC has been investigated in patients undergoing both partial-brain RT and WBRT using the diffusion tensor imaging (DTI), a MRI technique that offers a quantitative measure of WM damage [38-41]. Among the different examined regions of the brain, the most prominent dose-dependent changes after RT were found in the posterior part of the cingulum, in the fornix, in the corpus callosum and in the hippocampus [38-41]. Interestingly, the dose dependent progressive WM damage was observed [38-41] at time points early after RT [39]. Obviously, the knowledge of the regions with the most sensitivity to RT injury would facilitate the implementation of a more effective cognitive-sparing RT approach. Although the recommended LC dose constraints are not currently known, the correlation between radiation injury, LC and cognitive dysfunction has been demonstrated [38-41]. The progressive changes in the diffusivities and in the DTI index of the

posterior cingulum and the fornix found up to 6 months after partial-brain RT were related with memory function decline 18 months post-RT [41,42]. Interestingly, the vulnerability of the LC in relation to post-RT structural and functional alterations has been also observed in patients undergoing RT for NPC. The radiation damages of some brain networks including the LC was found in the late-delayed period after RT [43]. All these findings support the need to include all anatomical contributors to cognitive dysfunction within RT plans. A limitation in the pursuit of such strategy is the lack of an available contouring guide of LC. This is the essential fact that encouraged us to realize the first radiation oncologist's guide for delineation of the LC for its use in an everyday clinical practice and for an educational context. This MRI atlas provides a stepwise contouring guide with the specific definitions of the anatomic boundaries which may provide the basis for prospective studies on the quantification of dose-volume toxicity relationship for the LC. The study of these clinical and dosimetric aspects is a key element in the prediction of toxicity of the integrated oncological treatments. This study has significant limitations. The MRI scans were obtained from an individual with no oncological disease. However this is a common limit of all contouring atlas which are developed on imaging scans from healthy individuals. Additionally, this atlas does not describe post-surgery anatomy or anatomical variants. Finally, no test-re test analysis has been performed in order to investigate the intra-observer variability in the contouring of the different limbic structures.

5. Conclusions

This article provides step-by-step recommendations for the contouring of the LC in the setting of patients receiving radiation treatment. A complex relationship exists between the individual structures of the LC and radiation dose. Therefore, incorporation of all anatomical contributors to cognitive dysfunction within radiotherapy plans can be of clinical importance in reducing inappropriate dose to normal tissues.

Declarations of interest
None

Funding source

This research did not receive any specific grant from funding agencies in the public, commercial, or not-for-profit sectors.

References

1. Kazda T, Jancalek R, Pospisil P, et al. Why and how to spare the hippocampus during brain radiotherapy: the developing role of hippocampal avoidance in cranial radiotherapy. *Radiat Oncol* 2014; 6;9:139.
2. Pazzaglia S, Briganti G, Mancuso M, et al. Neurocognitive Decline Following Radiotherapy: Mechanisms and Therapeutic Implications. *Cancers (Basel)* 2020;8;12 (1): 146.
3. Jacob J, Durand T, Feuvret L, et al. Cognitive impairment and morphological changes after radiation therapy in brain tumors: A review. *Radiother Oncol* 2018;128(2):221-228.
4. Raber J, Rola R, LeFevour A, et al. Radiation-induced cognitive impairments are associated with changes in indicators of hippocampal neurogenesis. *Radiat Res* 2004; 162(1):39–47.
5. Ajithkumar T, Price S, Horan G, et al. Prevention of radiotherapy-induced neurocognitive dysfunction in survivors of paediatric brain tumours: the potential role of modern imaging and radiotherapy techniques. *Lancet Oncol* 2017;18(2):e91-e100.
6. Hutchinson AD, Pfeiffer SM, Wilson C. Cancer-related cognitive impairment in children. *Curr Opin Support Palliat Ca*re 2017;11(1):70-75.
7. Lee AW, Kwong DL, Leung SF et al. Factors affecting risk of symptomatic temporal lobe necrosis: Significance of fractional dose and treatment time. *Int J Radiat Oncol Biol Phys* 2002;53:75– 85.

8. Gondi et al . Hippocampal-Sparing Whole Brain Radiotherapy: A "How-To" Technique, Utilizing Helical Tomotherapy and LINAC-based Intensity Modulated Radiotherapy. *Int J Radiat Oncol Biol Phys* 2010;78(4):1244-52.
9. Gondi et al . Hippocampal dosimetry predicts neurocognitive function impairment after fractionated stereotactic radiotherapy for benign or low-grade adult brain tumors. *Int J Radiat Oncol Biol P*hys. 2013; 1;85(2):348-54.
10. Torres IJ, Mundt AJ, Sweeney PJ et al. A longitudinal neuropsychological study of partial brain radiation in adults with brain tumors. *Neurology* 2003;60:1113–1118.
11. Monje ML, Mizumatsu S, Fike JR, et al: Irradiation induces neural precursor-cell dysfunction. *Nat Med* 2002, 8(9):955–962.
12. Cerhan JH, Butts AM,. Parsons MW, et al. Neurocognitive Changes: Principles and Practice. In Chang EL, Brown PD,. Lo SS, Sahgal A, Suh J, Adult CNS Radiation Oncology: Springer International Publishing 2018; 591-603.
13. Bodensohn R, Corradini S, Ganswindt U, et al. A prospective study on neurocognitive effects after primary radiotherapy in high-grade glioma patients. *International Journal of Clinical Oncology* 2015; 4: 642-650.
14. Adeberg S, Harrabi SB, Bougatf N, et al. Intensity-modulated proton therapy, volumetric-modulated arc therapy, and 3D conformal radiotherapy in anaplastic astrocytoma and glioblastoma. *Strahlenther Onkol* 2016; 192, 11: 770-779.
15. Canyilmaz E, Uslu GDH, Colak F, et al. Comparison of dose distributions hippocampus in high grade gliomas irradiation with linac-based imrt and volumetric arc therapy: a dosimetric study, SpringerPlus, 2015.
16. Cosinschi A, Coskun M, Negretti L, et al. A metastatic relapse associated with hippocampal dose sparing after whole-brain radiotherapy, *Acta Oncologica* 2014; 54,10: 1824-1826.

17. Tsai PF, Yang CC, Chuang CC, et al. Hippocampal dosimetry correlates with the change in neurocognitive function after hippocampal sparing during whole brain radiotherapy: a prospective study, *Radiation Oncology* 2015: 10, 1: 253.
18. Falco MD Giancaterino S, D'Andrea M, et al. Hippocampal sparing approach in fractionated stereotactic brain VMAT radio therapy: A retrospective feasibility analysis. *J Appl Clin Med Phys* 2018;19(1):86-93.
19. Di Carlo C, Trignani M, Caravatta L, et al. Hippocampal sparing in stereotactic radiotherapy for brain metastases: To contour or not contour the hippocampus? Cancer Radiother 2018; 22(2):120-125.
20. Kim Y, Kim SH, Lee JH, et al. Verification of Low Risk for Perihippocampal Recurrence in Patients with Brain Metastases Who Received Whole-Brain Radiotherapy with Hippocampal Avoidance. Cancer Res Treat. 2019; 51(2):568-575.
21. Harrabi SB, Bougatf N, Mohr A, et al. Dosimetric advantages of proton therapy over conventional radiotherapy with photons in young patients and adults with low-grade glioma. *Strahlenther Onkol* 2016;192(11):759-769.
22. Lautin A. *The Limbic Brain*. New York, NY, USA: Kluwer Academic/ Plenum; 2001.
23. Marsh JC, Gielda BT, Herskovic AM, et al. Sparing of the hippocampus and limbic circuit during whole brain radiation therapy: A dosimetric study using helical tomotherapy. *J Med Imaging Radiat Oncol* 2010; 54(4):375-82.
24. Marsh JC, Ziel GE, Diaz AZ, et al. Integral dose delivered to normal brain with conventional intensity-modulated radiotherapy (IMRT) and helical tomotherapy IMRT during partial brain radiotherapy for high-grade gliomas with and without selective sparing of the hippocampus, limbic circuit and neural stem cell compartment. *J Med Imaging Radiat O*ncol 2013;57(3):378-83;

25. Marsh JC, Godbole R, Diaz AZ, et al Sparing of the hippocampus, limbic circuit and neural stem cell compartment during partial brain radiotherapy for glioma: a dosimetric feasibility study. *J Med Imaging Radiat Oncol*. 2011;55(4):442-9.

26. Marsh JC, Herskovic AM, Gielda BT, et al. Intracranial metastatic disease spares the limbic circuit: a review of 697 metastatic lesions in 107 patients. *Int J Radiat Oncol Biol Phys* 2010; 76(2):504–512.

27. Gondi V, Tome WA, Marsh J, et al. Estimated risk of perihippocampal disease progression after hippocampal avoidance during whole-brain radiotherapy: safety profile for RTOG 0933. *Radiother Onc*ol 2010; 95(3):327–331.

28. Ghia A, Tomé WA, Thomas S, et al. Distribution of brain metastases in relation to the hippocampus: implications for neurocognitive functional preservation. *Int J Radiat Oncol Biol Phys* 2007; 68(4):971–977.

29. Hong AM, Suo C, Valenzuela M, et al. Low incidence of melanoma brain metastasis in the hippocampus. *Radiother Oncol* 2014; 111(1):59–62.

30. Sun B, Huang Z, Wu S, et al. Incidence and relapse risk of intracranial metastases within the perihippocampal region in 314 patients with breast cancer. *Radiother Oncol* 2016;118:181-6.

31. S Henri M. Duvernoy, The Human Hippocampus, Springer-Verlag Berlin Heidelberg 2005.

32. Jurgen K. Mai, Joseph Assheuer, George Paxinos; Atlas of the HUMAN BRAIN Atlas of the Human Brain - Elsevier Academic Press 525 B Street, Suite 1900, San Diego, California 92101-4495, USA 2003.

33. Ben Greenstein, Adam Greenstein; Color Atlas of Neuroscience: Neuroanatomy and Neurophysiology; Thieme, Stuttgart · New York 2011.

34. Sharma A. App review series: e-Anatomy. J Digit Imaging 2015;28:256–8.

35. Destrieux C, Fischl B, Dale A, et al. Automatic parcellation of human cortical gyri and sulci using standard anatomical nomenclature. *Neuroimage* 2010;53(1):1-15.

36. Destrieux C, Terrier LM, Andersson F, et al. A practical guide for the identification of major sulcogyral structures of the human cortex. *Brain Struct Funct* 2017;222(4):2001-2015.
37. Nazem-Zadeh MR, Chapman CH, Lawrence TL, et al. Radiation therapy effects on white matter fiber tracts of the limbic circuit. *Med Phys* 2012;39(9):5603-13.
38. Connor M, Karunamuni R, McDonald C, et al. Regional susceptibility to dose-dependent white matter damage after brain radiotherapy. *Radiother Oncol.* 2017;123(2):209-217.
39. Chapman CH, Nazem-Zadeh M, Lee OE, et al. Regional variation in brain white matter diffusion index changes following chemoradiotherapy: a prospective study using tract-based spatial statistics. *PLoS One* 2013;8(3):e57768.
40. Nazem-Zadeh M, Chapman C, Lawrence T, et al. WE-G-217A-04: Segmenting Limbic Circuit Fiber Tracts for Quantifying Changes in Diffusion Indices Due to Partial Radiation Therapy. *Med Phys* 2012;39(6Part28):3975-3976.
41. Chapman H, Nagesh V, Sundgren P, et al. "Diffusion tensor imaging of normal-appearing white matter as biomarker for radiation-induced late delayed cognitive decline," *Int. J. Radiat. Oncol., Biol., Phys* 2012; 82(5), 2033–2040.
42. Oishi K, Lyketsos CG. Alzheimer's disease and the fornix. Front Aging Neurosci 2014;6:1–9.
43. Chen Q, Lv X, Zhang S, et al. Altered properties of brain white matter structural networks in patients with nasopharyngeal carcinoma after radiotherapy. *Brain Imaging Behav* 2020 Jan 3 Online ahead of print.

Biographies

Claudia Sorce attended Medical School at the University of Palermo (Italy). After her graduation she started working as a resident in Radiotherapy at the Department of Biotechnological and Applied Clinical Sciences (Division of Radiotherapy and Radiobiology, University) of the University of L'Aquila. In 2019, she successfully defended her thesis on the post-RT toxicity of the limbic system in subjects treated for primary and secondary brain tumors. Head and Neck cancer treatment is an additional field of particular interest.

Agnieszka Chalaszczyk attended Medical School at the Pomeranian Medical University in Szczecin (Poland). Form November 2016 to October 2020 she attended as resident in Radiotherapy at the Department of Biotechnological and Applied Clinical Sciences (Division of Radiotherapy and Radiobiology, University) of the University of L'Aquila. In 2020 she finished her training at the National Institute for Tumors "Pascale Foundation" of Naples in the Department of Radiation Oncology (Subdivision of CyberKnife). Head and Neck cancer treatment is her field of particular interest. She currently works as at the Clinical Department of the National Center for Oncological Hadrontherapy (CNAO) of Pavia. In this position her scientific fields include the radiation treatment of sarcoma with heavy ions.

Francesca Rossi attended Medical School at the Catholic University of the Sacred Heart (Rome). After her graduation she started working as a resident in Radiotherapy at the Department of Biotechnological and Applied Clinical Sciences (Division of Radiotherapy and Radiobiology, University) of the University of L'Aquila. Post-RT toxicity of the limbic system in subjects treated for primary and secondary brain tumors and the Head and Neck cancer treatment are the two main fields of particular interest.

Letizia Ferella attended Medical School at the University of L'Aquila (Italy). After her graduation she started working as a resident in Radiotherapy at the Department of Biotechnological and Applied Clinical Sciences (Division of Radiotherapy and Radiobiology, University) of the University of L'Aquila. In 2018 she finished her training at the National Institute for Tumors of Milan in the Department of Radiation Oncology (Subdivision of Head and Neck cancer). Head and Neck cancer treatment is her field of particular interest. She currently works as at the Radiation Oncology Department of the Aosta Hospistal, in the ThomoTherapy Unit. In this position her scientific fields include the radiation treatment of brain and head and neck tumors.

Gianmarco Grimaldi attended Medical School at the "La Sapienza" University (Rome). After his graduation he started working as a Ph.D. student at the "La Sapienza" University on a collaborative research project on the treatment of the gastrointestinal tumors. After his Ph.D., he started working as a resident in Radiotherapy at the Department of Biotechnological and Applied Clinical Sciences (Division of Radiotherapy and Radiobiology, University) of the University of L'Aquila. Post-RT toxicity of CNS in subjects treated for primary and secondary brain tumors and the Head and Neck cancer treatment are the two main fields of his particular interest. He currently works as at the Radiation Oncology Department of the UPMC HILLMAN CANCER CENTER SAN PIETRO FBF (Rome).

Alessandra Splendiani is an Associate Professor in Neuroradiology at the Department of Biotechnological and Applied Clinical Sciences of University of L'Aquila (Italy). She currently is

consultant in the University Division of Neuroradiology and her field of scientific interest includes the advanced and functional Imaging in neuro-oncology.

Domenico Genovesi currently is an Associate Professor in Radiotherapy at the Department of Neuroscience, Imaging and Clinical Science of the G. D'Annunzio' University (Chieti, Italy). He currently is the head of the University Division of Radiotherapy and his field of scientific interest includes the radiation treatment of gastrointestinal tumors and the radiological contouring of target volumes and organs at risk.

Francesco Marampon attended Medical School at the University of L'Aquila (Italy). After his graduation he started working as a Ph.D. student at the Department of Biotechnological and Applied Clinical Sciences of University of L'Aquila (Italy) on a collaborative research project on the radiobiology of the solid tumors. After his Ph.D., he started working as a resident in Radiotherapy at the Department of Biotechnological and Applied Clinical Sciences (Division of Radiotherapy and Radiobiology, University) of the University of L'Aquila. He currently is an Assistant Professor in Radiotherapy at the Department of Radiation Oncology of the Policlinico Umberto I Hospital (Sapienza, University of Rome, Italy)

Ester Orlandi attended Medical School at the University of Milan (Italy). After her graduation she started working as a resident student at the Department of Radiotherapy of the University of Milano-Bicocca (Italy). From 2008 to 2017 he worked as consultant Radiotherapists at The National Cancer Institute of Milan in the Department of Radiation Oncology. On April 2018 she obtained the Italian Scientific License for Associate Professorship in Radiotherapy. From 2018 to February 2020 she obtained an appointment for Head and Neck Cancer highly Specialized Radiation Oncologist. From March 2020 she is the Director of the Clinical Department of the National Center for Oncological Hadrontherapy (CNAO) (Pavia, Italy).

Alberto Iannalfi attended Medical School at the University of Florence (Italy). After his graduation he started working as a resident student at the Department of Radiotherapy of the University of Florence (Italy). From 2009 to 2010 he worked as consultant Radiotherapists at the European Institute of Oncology (Milan, Italy). From June 2010 he currently works as consultant Radiotherapist at the Clinical Department of the National Center for Oncological Hadrontherapy (CNAO) (Pavia, Italy).

Carlo Masciocchi is a Full Professor in Radiology and Radiotherapy at the Department of Biotechnological and Applied Clinical Sciences of University of L'Aquila (Italy). He currently is the Director of the University Division of Radiology and Radiotherapy. His field of scientific interest also includes the advanced and functional Imaging in Musculoskeletal and neuro-oncology.

Giovanni Luca Gravina attended Medical School at the University of L'Aquila (Italy). After his graduation he started working as a resident in Radiotherapy at the Department of Biotechnological and Applied Clinical Sciences (Division of Radiotherapy and Radiobiology, University) of the University of L'Aquila. After his specialization in radiotherapy he started working as a Ph.D. student at the Department of Experimental Medicine of the "La Sapienza" University (Rome, Italy) on a collaborative research project on the radiobiology of the solid tumors. He currently is an Associate Professor in Radiotherapy at the Department of Biotechnological and Applied Clinical

Sciences of University of L'Aquila (Italy) and from June 2016 he works as consultant Radiotherapist.

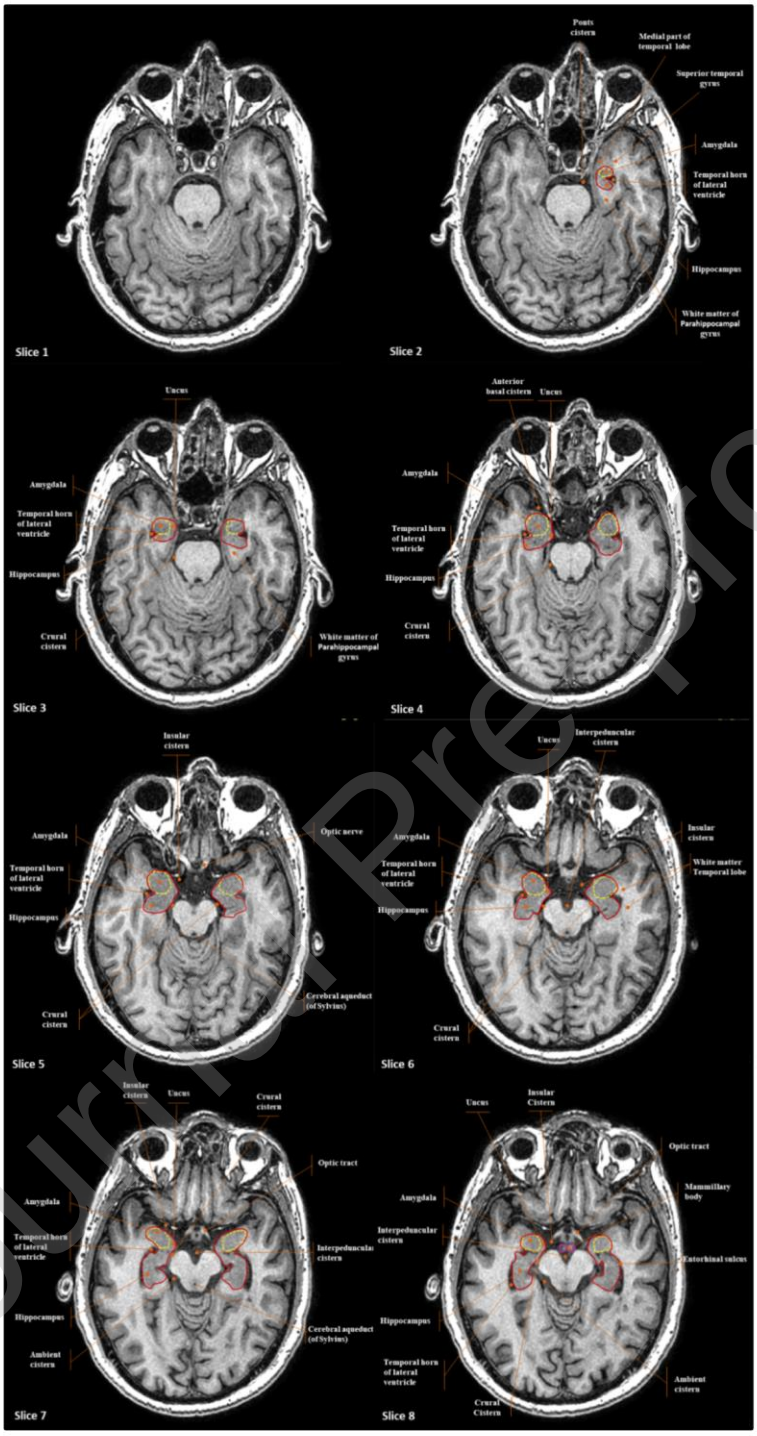

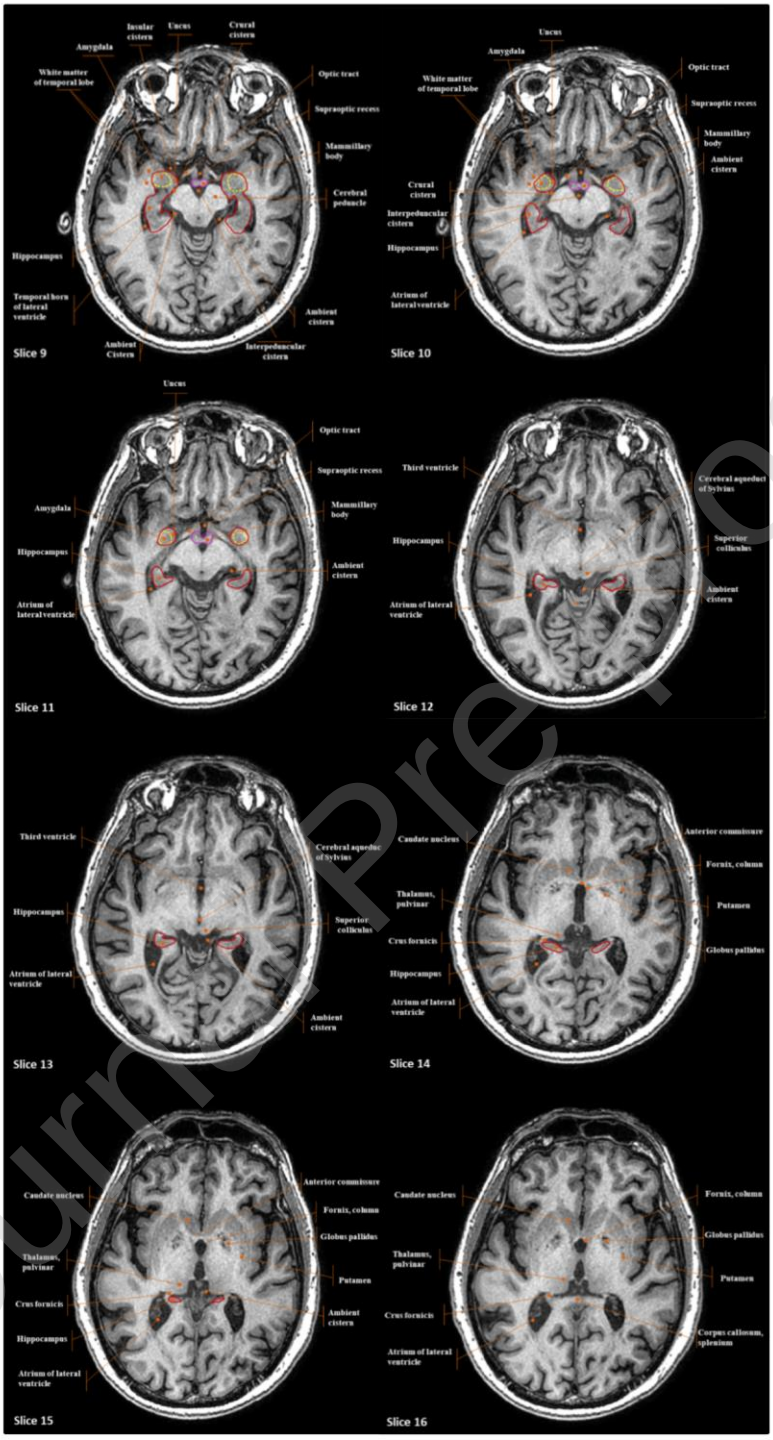

Figure 1: Representative view of the hippocampal-amygdala formation and mammillary bodies contoured on an axial plane.

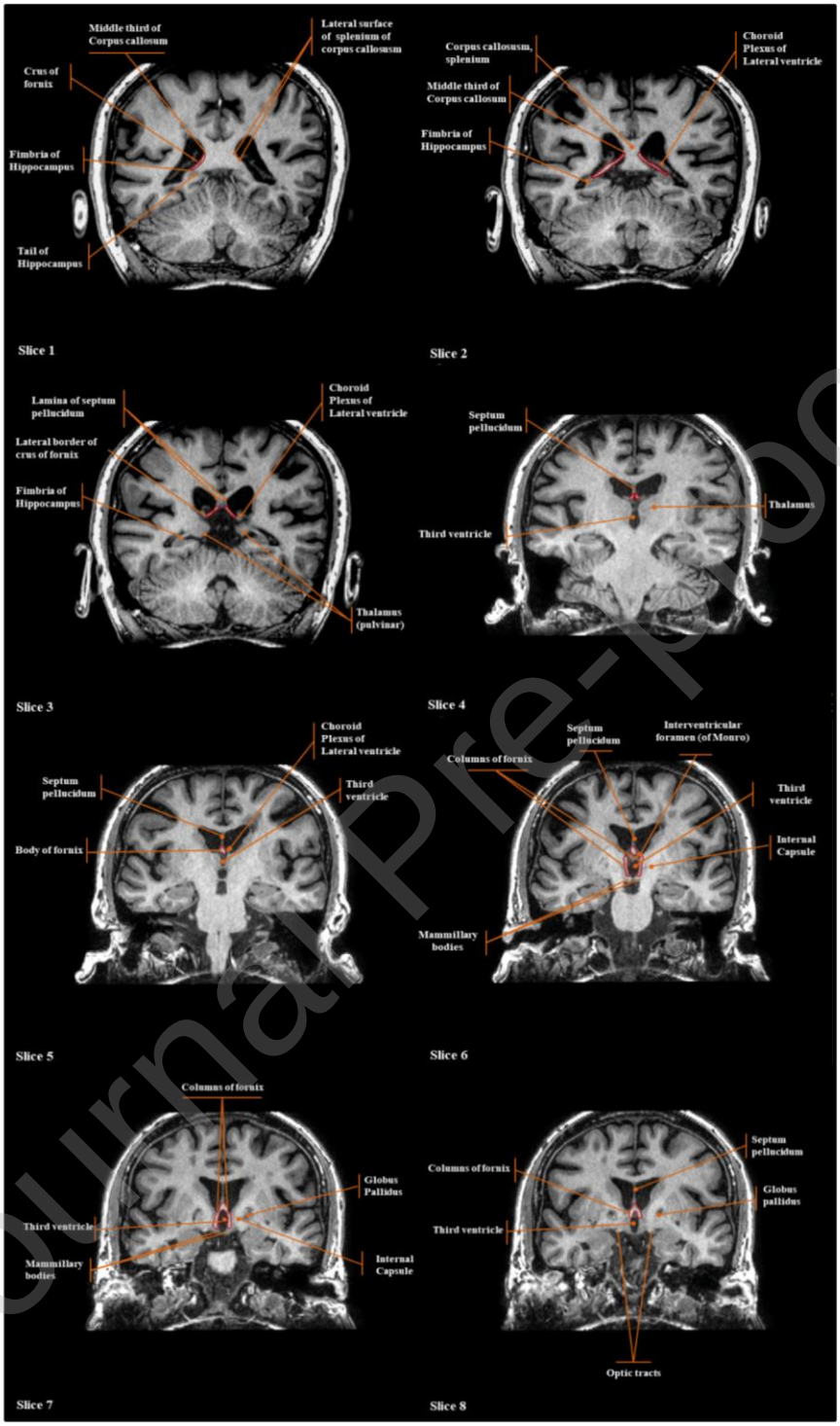

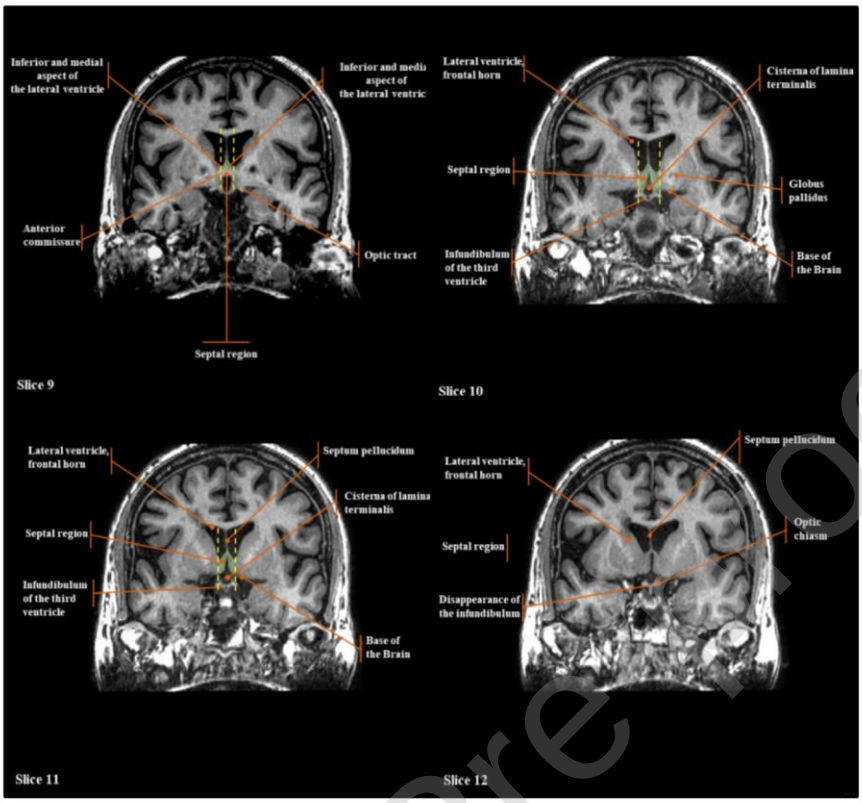

Figure 2: Representative view of the fornix and septal region contoured on a coronal plane.

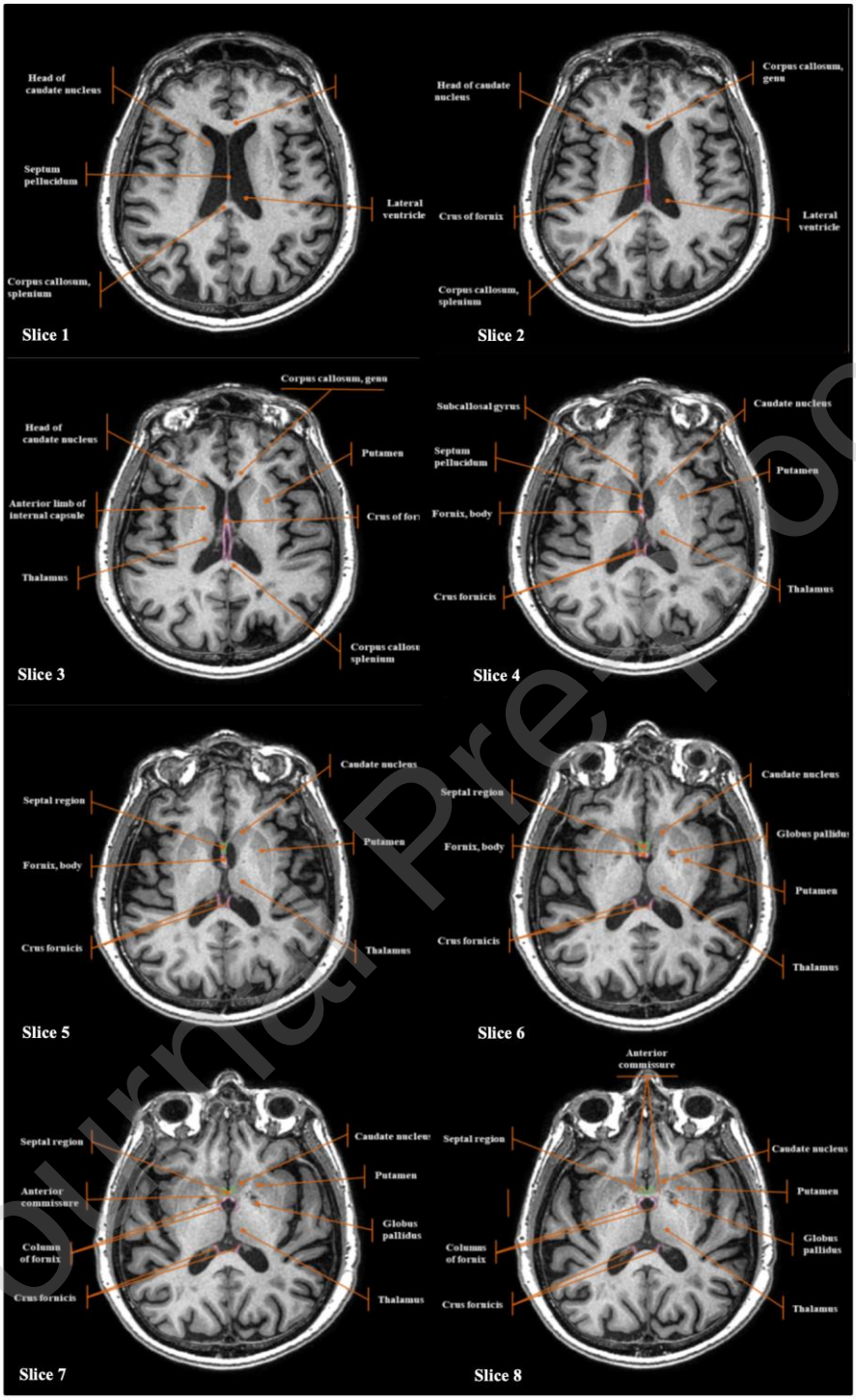

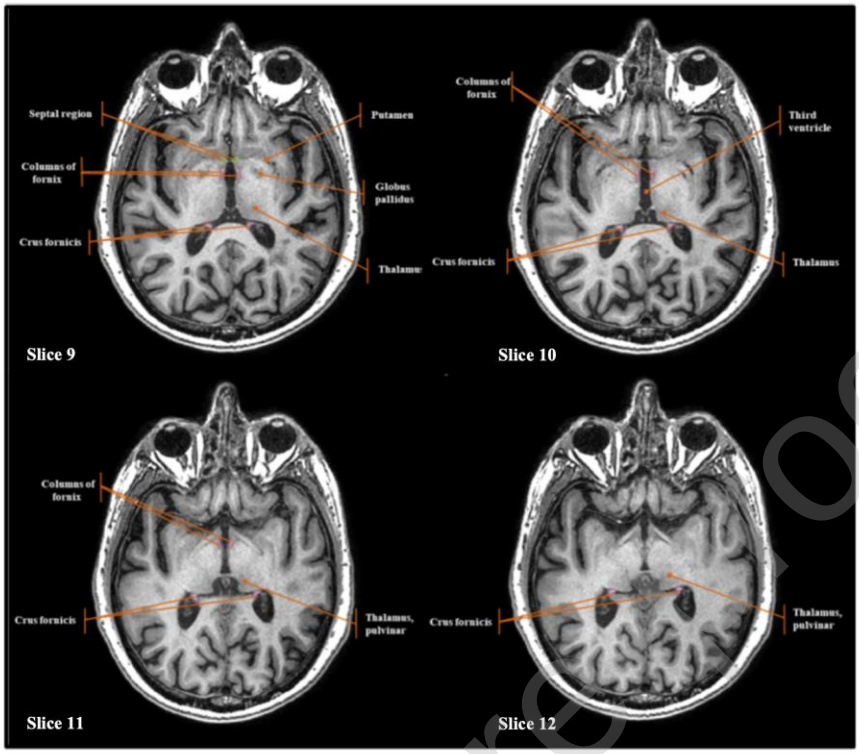

Figure 3: Representative view of the fornix and septal region contoured on an axial plane.

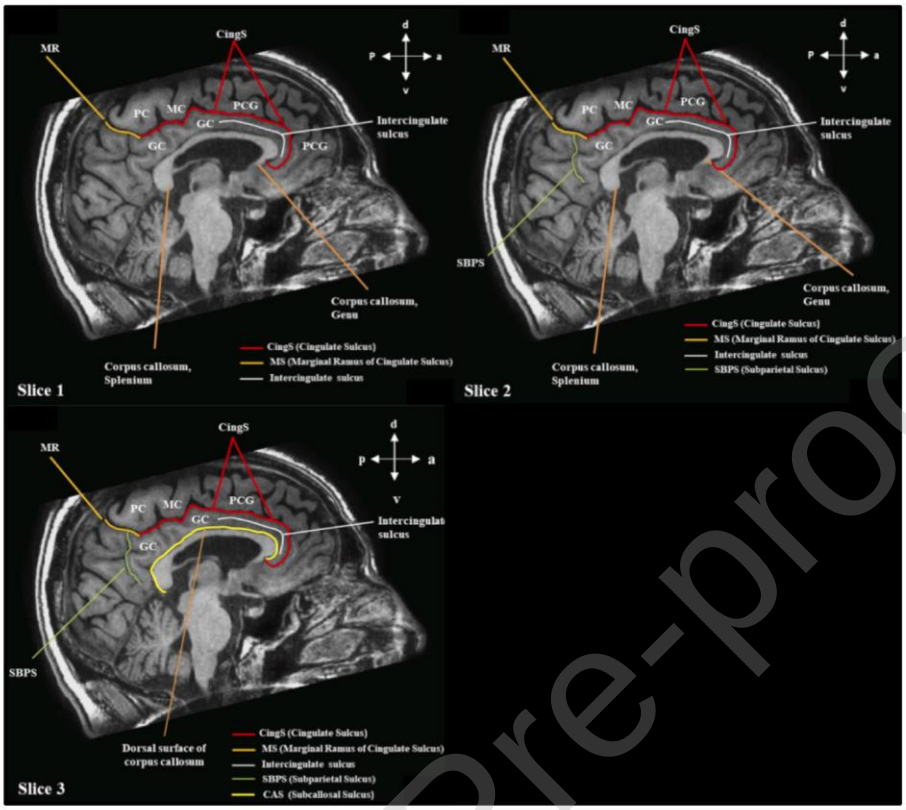

Figure 4: Representative view of the sulci bordering the CG contoured on a sagittal plane.

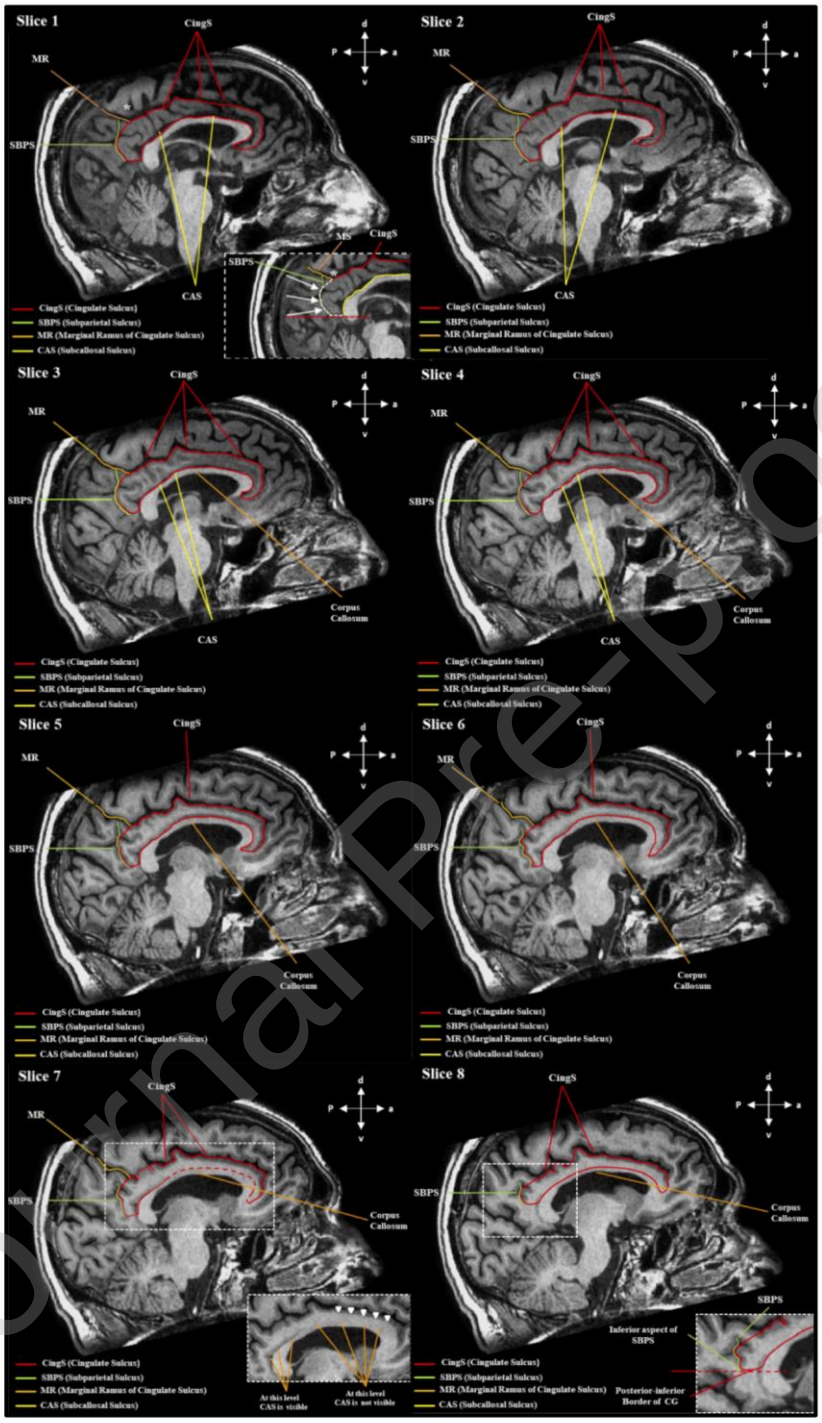

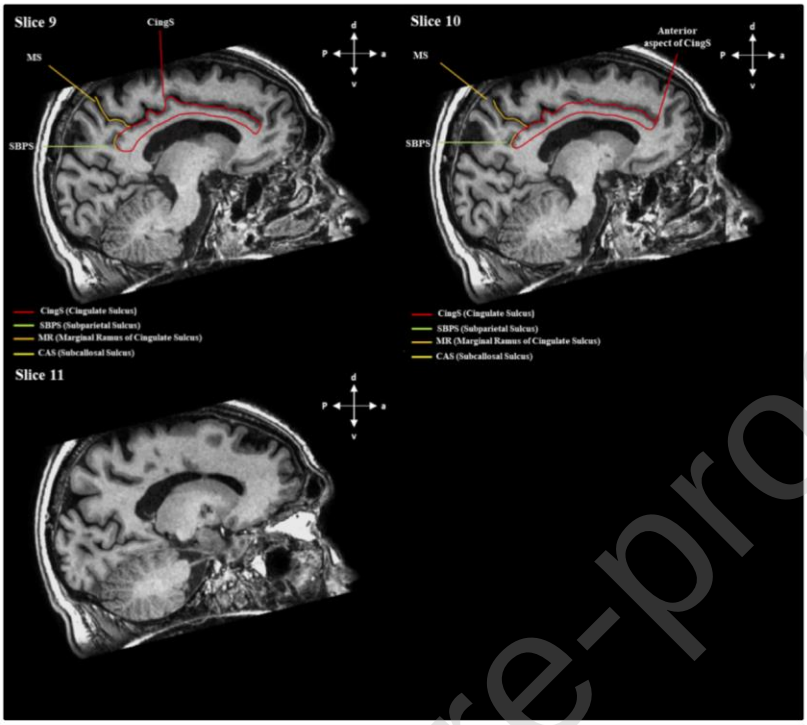

Figure 5: Representative view of the CG contoured on a sagittal plane.

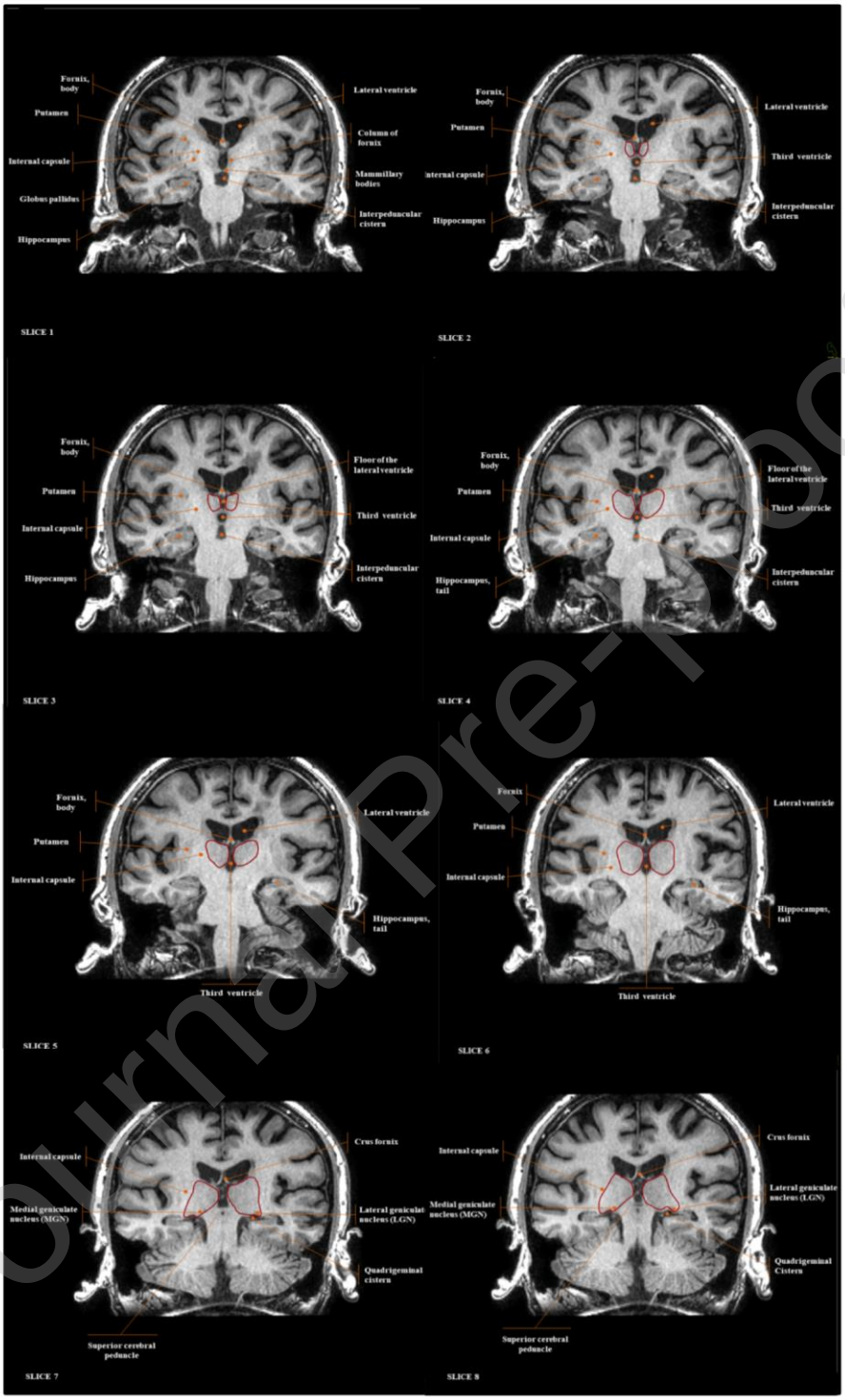

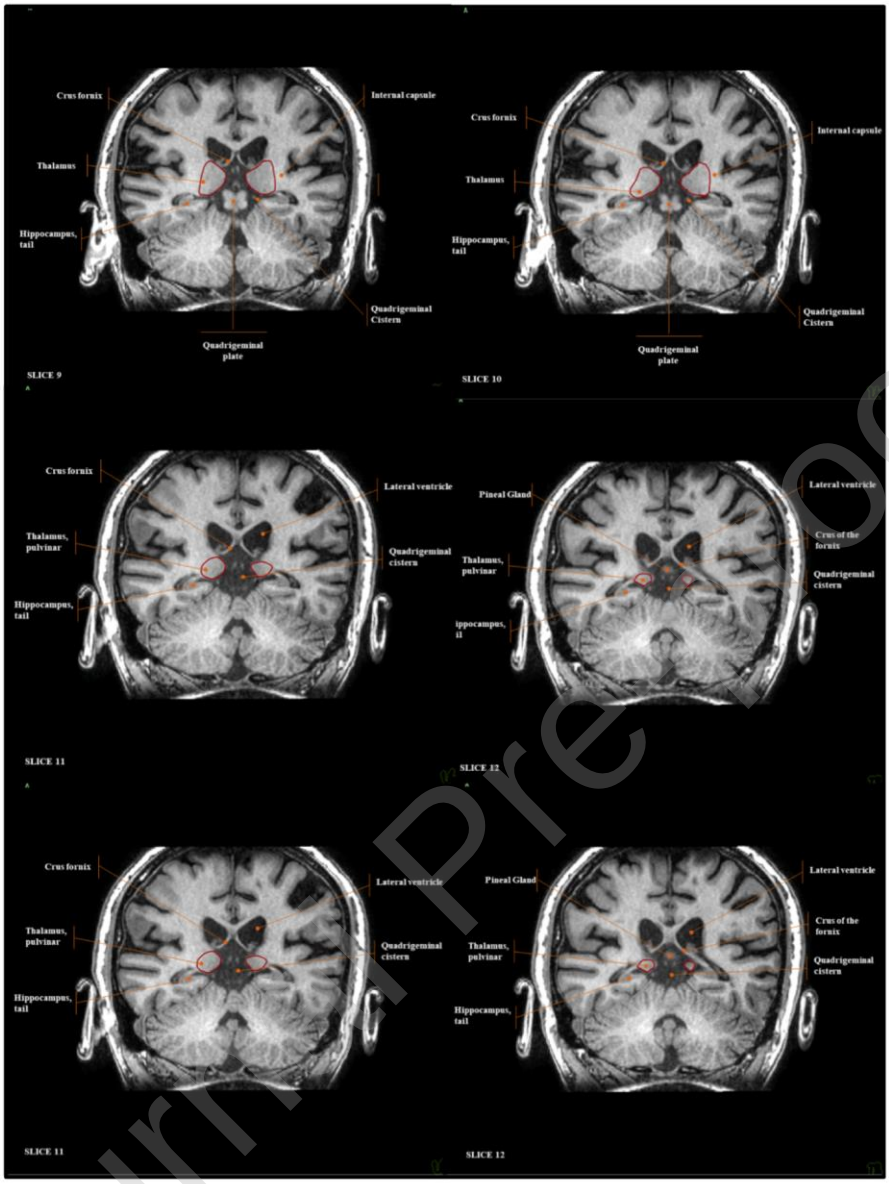

Figure 6: Representative view of the thalamus contoured on a coronal plane.

Figure 7: Representative view of the thalamus contoured on an axial plane.